A Nuclear Magnetic Resonance Study of Sulphur and Selenium Inversion in Complexes of Trimethylplatinum(IV) Halides with Dithio- and Diseleno-ethers

By Edward W. Abel, A. Rauf Khan, Kenneth Kite, Keith G. Orrell,* and Vladimir Šik, Department of Chemistry, University of Exeter, Exeter, Devon EX4 4QD

Dynamic n.m.r. studies have yielded accurate energy data for S and Se pyramidal inversion in complexes of type $[PtXMe_3(L\text{–}L)]$ [X = Cl, Br, or I; L–L = $MeE(CH_2)_nEMe$, E = S or Se, n = 2 or 3]. The mechanism of the inversion process and the effects of atomic mass, ring size, and nature of halogen on the barrier energies are discussed.

THE study of pyramidal inversion of nitrogen atoms has become a classic example [1] of the dynamic n.m.r. (d.n.m.r.) technique and over the past 20 years or so a considerable wealth of data (of variable accuracy) on the energetics of this process has been collated and critically assessed.[2-4] Data for other inverting atoms, however, are relatively sparse due basically to a mismatching of the inversion rates of other pyramidal atoms with the observational time scale of the n.m.r. technique. Thus, other Group 5A elements exist, in general, in pyramidal configurations too stable for n.m.r. studies whereas with Group 6A elements, oxygen tends to invert too rapidly and sulphur, selenium, and tellurium too slowly with respect to the n.m.r. time scale. However, we [5-7] and other workers [8-11] have shown that bonding of S, Se, or Te to transition metals accelerates the inversion rate and makes it very amenable to n.m.r. detection.

As part of a comprehensive investigation of the factors governing the energy barriers of ring and pyramidal site inversion processes of Group 6A atoms we report here our studies on the complexes $[PtXMe_3(L\text{–}L)]$ [X = Cl, Br, or I; L–L = $MeE(CH_2)_nEMe$, E = S or Se, n = 2 or 3]. We have shown elsewhere [12,13] that in these complexes the ligands (L–L, n = 2 or 3) act as normal bidentate S or Se donors in contrast to the ligands (L–L, n = 0 or 1) which act as bridging ligands between pairs of Pt atoms. Variable-temperature n.m.r. studies of the above complexes clearly reveal the presence of internal dynamic processes. In the case of the five-membered ring complexes (n = 2), the only likely rate process to come within the frequency range of n.m.r. detection is pyramidal inversion of the pairs of S or Se atoms either independently or synchronously. The five-membered ring puckering vibration [14] is expected to be too rapid for n.m.r. detection in the temperature range studied. In the case of the six-membered ring complexes (n = 3), both ring reversal and pyramidal site inversion processes are possible causes of the n.m.r. line-shape changes with temperature. We show here how total band-shape fitting methods have provided reliable energy data for these spectral changes and to which particular processes these data are attributed.

EXPERIMENTAL

Materials.—All the complexes discussed here were prepared by the general method previously described.[13] The complexes were soluble in a variety of organic solvents, deuteriochloroform (>99.8% D) being used as the n.m.r. solvent whenever possible.

Spectra.—N.m.r. spectra were obtained using either a JEOL MH-100 100 MHz spectrometer operating in the continuous-wave mode under internal field–frequency lock conditions or a JEOL PS/PFT-100 spectrometer operating in the Fourier-transform mode at 100 MHz for ^1H studies. A JES-VT-3 variable-temperature unit was used to control the probe temperature. Temperature measurements were made immediately before and after recording spectra using a precisely calibrated copper–constantan thermocouple. All temperatures quoted are considered accurate to ≤1 °C.

Computations.—The computer program DNMR developed by Kleier and Binsch [15] was used as the basis of the band-shape calculations. The original program was modified [6] in order to compute spin systems interconverting between more than three chemical configurations. Matchings of theoretical and experimental spectra (using suitably expanded traces) were performed by eye. Despite the subjectivity of the method, visual matchings were found to be most reliable for complex changes of line shape, a conclusion in accord with that recently expressed by Binsch and co-workers.[16]

RESULTS

The five-membered ring complexes $[PtXMe_3\{MeE(CH_2)_2EMe\}]$ will be discussed first. The two S or Se atoms are centres of chirality and thus, in the absence of any internal rate process, four diastereoisomers of these complexes may exist, namely two distinct *meso* forms and a degenerate pair of DL forms (Figure 1). Evidence for these invertomers comes from the low-temperature spectra of these complexes. The spectra of $[PtIMe_3\{MeS(CH_2)_2SMe\}]$ which may be taken as typical of other complexes in the series are illustrated in Figure 2. At *ca.* −35 °C, the S–Me region consists of four lines (plus ^{195}Pt satellite lines) which are attributed to the three distinct invertomers (Figure 1). On warming the sample, coalescence of these signals occurs until at *ca.* 65 °C a single averaged line (plus ^{195}Pt satellites) is observed. These changes are without doubt due to the varying rate of pyramidal inversion at the sulphur atoms. Supporting evidence for these three invertomers comes from the Pt–Me region of the spectrum where seven signals (three for methyls *trans* to halogen and four for methyls *trans* to S) are expected and indeed observed for the complexes $[PtXMe_3\{MeSe(CH_2)_2SeMe\}]$ (X = Cl, Br, or I). In the corresponding sulphur ligand complexes only five or six signals were observed due to fortuitous chemical-shift overlaps. The chemical-shift and spin–spin coupling-constant data for the Pt–Me signals are collected in Table 1 where the low-temperature data refer to the individual

invertomers, and the high-temperature data represent weighted averaged invertomer values. It will be noted that the individual invertomers of the sulphur ligand complexes differ in the chemical shifts of Pt–Me (*trans* E) and Pt–Me (*trans* X) by 0.06—0.08 p.p.m. and 0.09—0.12 p.p.m. respectively. Somewhat greater shift differences were evident in the corresponding selenium complexes. No attempt was made to assign individual Pt–Me lines to individual invertomers.

The methylene regions of the spectra of all the complexes exhibited predictably complex absorptions at most temperatures and were not analysed in any detail as no additional information would have been obtained.

Returning to the S–Me region, the assignments of the lines as shown in Figure 2 and Table 2 were made on the basis of the observed trends in the chemical shifts, the ^3J(Pt–H) values, and the invertomer populations. The pair of signals at higher field with relatively larger values of ^3J(Pt–H) were assigned to the methyl C (DL-1,2 isomers) and the methyls DD′ (*meso*-2 isomer), the latter being the

TABLE 1

Chemical shifts and spin coupling constants of Pt–Me protons in the slow and fast inversion limits

		PtMe (*trans* to E)		PtMe (*trans* to X)	
Complex	θc/°C	δ/p.p.m.	^2J/Hz	δ/p.p.m.	^2J/Hz
(1) [$PtClMe_3\{MeS(CH_2)_2SMe\}$]	45.3	1.22	69.9	0.78	73.2
	−49.5	1.16, 1.23, 1.24	69.3, 69.0, 69.0	0.74, 0.86	73.9, 73.8
(2) [$PtBrMe_3\{MeS(CH_2)_2SMe\}$]	26.0	1.28	69.9	0.84	72.5
	−64.0	1.25, 1.30, 1.33	69.3, 69.3, 69.3	0.82, 0.93	71.9, 71.9
(3) [$PtIMe_3\{MeS(CH_2)_2SMe\}$]	64.8	1.50	71.0	0.98	69.8
	−55.8	1.38, 1.40, 1.40, 1.44	69.8, 69.8, 69.3, 69.8	0.91, 1.00	70.6, 70.3
(4) [$PtClMe_3\{MeSe(CH_2)_2SeMe\}$]	104.3	1.31	69.8	0.76	73.1
	0.4	1.25, 1.29, 1.34, 1.35	69.6, 69.4, 69.6, 69.3	0.68, 0.73, 0.87	73.9, 73.9, 73.6
(5) [$PtBrMe_3\{MeSe(CH_2)_2SeMe\}$]	104.3	1.41	70.6	0.84	72.5
	−1.4	1.34, 1.37, 1.40, 1.42	69.9, 69.6, 69.6, 69.6	0.79, 0.82, 0.95	73.9, 73.4, 72.5
(6) [$PtIMe_3\{MeSe(CH_2)_2SeMe\}$]	100.0	1.56	70.9	0.95	70.5
	−21.0	1.51, 1.51, 1.53, 1.57	70.5, 70.5, 70.0, 70.3	0.93, 0.94, 1.04	70.9, 70.9, 70.3
(7) [$PtClMe_3\{MeS(CH_2)_3SMe\}$]	r.t.*	1.00	68.7	0.85	72.2
	−74.1	0.93, 0.96, 1.03	68.1, 68.8, 67.6	0.80, 0.95	72.6, 72.3
(8) [$PtBrMe_3\{MeS(CH_2)_3SMe\}$]	r.t.*	1.09	69.0	0.98	71.4
	−67.4	1.02, 1.04, 1.12	68.2, 69.3, 67.6	0.92, 1.08	72.2, 71.9
(9) [$PtIMe_3\{MeS(CH_2)_3SMe\}$]	r.t.*	1.23	69.4	1.15	70.0
	−60.0	1.16, 1.17, 1.28	68.8, 69.9, 68.2	1.08, 1.23	69.9, 69.7
(10) [$PtClMe_3\{MeSe(CH_2)_3SeMe\}$]	63.5	1.18	69.3	0.92	72.9
	−24.1	1.11, 1.15, 1.21	68.9, 69.6, 68.1	0.91, 1.05	73.5, 73.3
(11) [$PtBrMe_3\{MeSe(CH_2)_3SeMe\}$]	64.3	1.25	69.6	1.02	72.2
	−32.0	1.17, 1.21, 1.29	68.2, 69.7, 68.8	1.01, 1.17	72.8, 72.5
(12) [$PtIMe_3\{MeSe(CH_2)_3SeMe\}$]	80.0	1.39	70.2	1.17	69.6
	−21.0	1.30, 1.31, 1.45	68.6, 70.3, 68.7	1.15, 1.32	70.4, 70.3

* Room temperature not measured precisely.

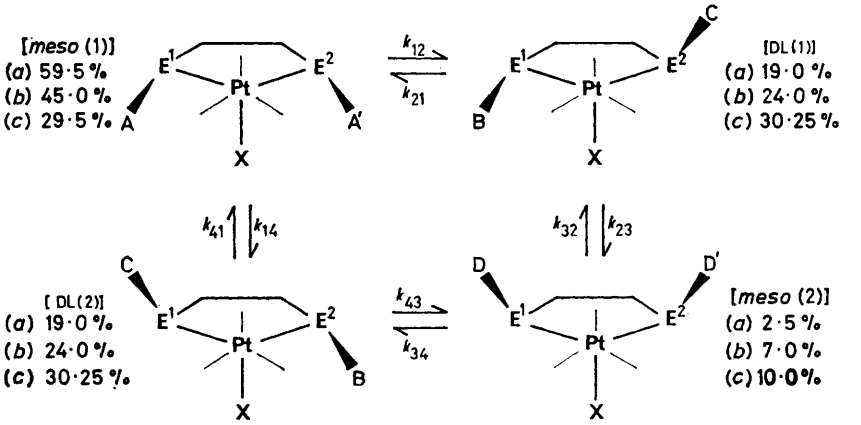

FIGURE 1 Interconversion of *meso* and DL isomers of [$PtXMe_3\{MeE(CH_2)_2EMe\}$] by independent inversion of E atoms. Percentage populations refer to the complex E = S, (*a*) X = Cl, (*b*) X = Br, (*c*) X = I and were essentially temperature independent

lower intensity signal (Figure 2). The lower-field bands were accordingly assigned to the methyls AA′ (*meso*-1 isomer) and methyl B (DL-1,2 isomers). Such assignments are based on the observation that hydrogens situated nearer the plane containing the E–Pt and equatorial Me–Pt

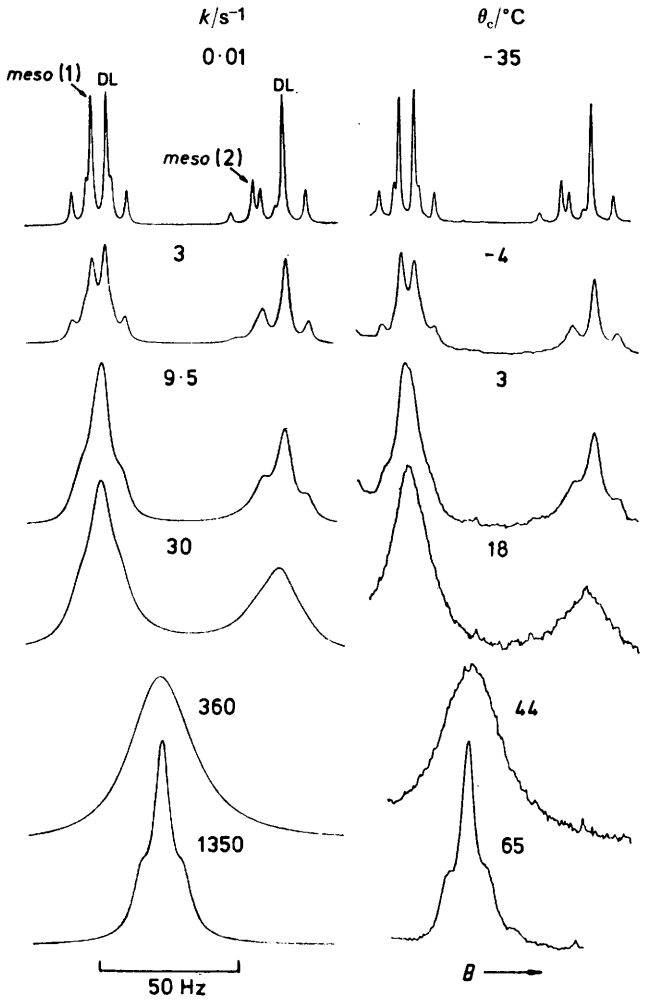

FIGURE 2 Variable-temperature ^1H n.m.r. spectra of the SMe region of $[PtIMe_3\{MeS(CH_2)_2SMe\}]$ and the computer-simulated spectra

bonds exhibit lower δ values and higher ^3J values.[8,9,17–20] In these complexes the methyls DD′ (*meso*-2) and C (DL-1,2) are nearer the E–Pt–E plane and thus appear at higher field and with larger magnitudes of ^3J than the methyls AA′ (*meso*-1) and B (DL-1,2). The latter, being situated below the average E–Pt–E plane, are very sensitive to the nature of the halogen. For example, in the series $[PtXMe_3\{MeS(CH_2)_2SMe\}]$ when X varies from Cl to I, the chemical shift δ_A increases by 18.6 Hz at *ca.* 0 °C whereas δ_C increases by only *ca.* 0.5 Hz. Furthermore, increasing the size of the halogen appeared to favour the less sterically restricted *meso*-2 and DL isomers at the expense of the *meso*-1 isomer, such that in the iodo-complex the DL isomers become the most abundant of all (Figures 1 and 3). In other cases, the invertomer populations were in the sequence *meso*-1 > DL-1 = DL-2 ≫ *meso*-2.

When pyramidal inversion becomes rapid, the different environments of the E–Me groups become averaged. This is illustrated by the cyclic scheme (Figure 1) where inversion is considered to occur at each E atom independently in an uncorrelated manner. Commencing with *meso*-1, where both methyls are isochronous, inversion at E^2 leads to the DL-1 invertomer with a rate constant k_{12}. Inversion at E^1 in *meso*-1 produces the DL-2 invertomer which differs from DL-1 only in the labelling of the methyls. Inversion at E^2 in DL-2 or at E^1 in DL-1 produces the *meso*-2 invertomer where both methyls are again isochronous. Due to the likely low probability of synchronous inversion of both E atoms, direct interconversion between *meso*-1 and *meso*-2 and between DL-1 and DL-2 was neglected at this stage,

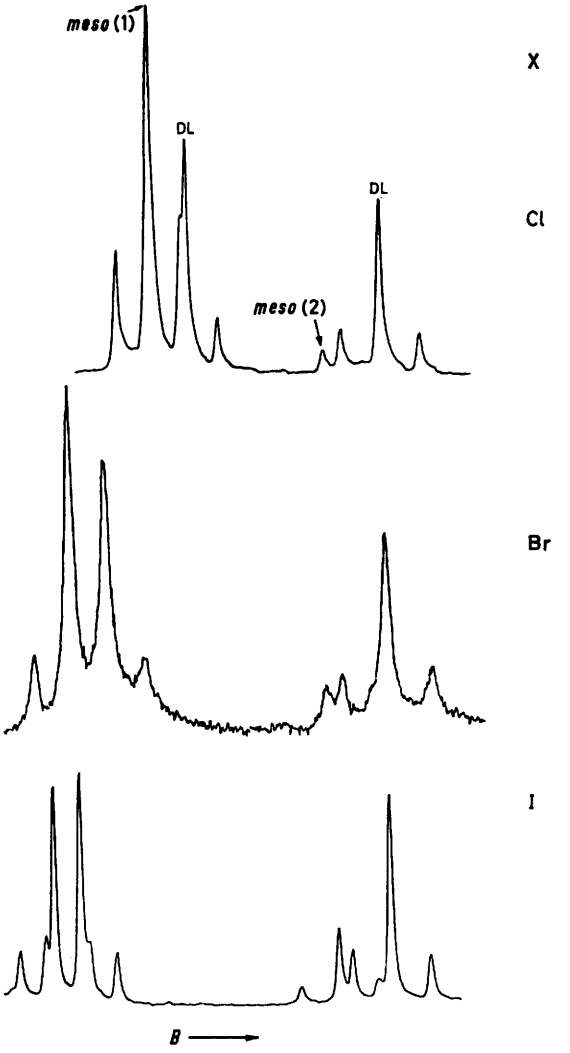

FIGURE 3 Low-temperature ^1H n.m.r. spectra of $[PtXMe_3\{MeS(CH_2)_2SMe\}]$ showing the invertomer population dependence of X. Note that the spectra were recorded at slightly different horizontal scale expansions and the spectra are arbitrarily aligned with respect to the high-field DL-isomer signal

i.e. k_{13} and k_{24} were equated to zero. Now it is necessarily true that $k_{12} = k_{14}$ and that $k_{23} = k_{34}$. However, in view of the structural similarities of all four invertomers, it was further assumed that these four rate constants were all equal. This is an assumption which cannot be fully justified

on rigorous kinetic grounds, but which seems highly reasonable and is mathematically desirable in order to avoid too many line-shape fitting variables. It should be noted, however, that since the populations of the *meso* and DL isomers are unequal, that in general the rate constants $k_{ij} \neq k_{ji}$. This follows from the general relation (1) where p_i refers to the population of isomer i.

$$p_i k_{ij} = p_j k_{ji} = k \quad (1)$$

Thus, the dynamic process under investigation involves interconversion between four distinct chemical configurations each consisting of two spins. In addition, allowance has to be made for the spin coupling between ^{195}Pt (33.7% natural abundance) and the E methyls. Thus, the total spin system is as in Scheme 1. For the reasons given above,

SCHEME 1

all the configurations were related to contiguous configurations by the same rate constant, k. Since no spin coupling was observed between E methyls in the same isomer, the spin problem could be simplified to Scheme 2.

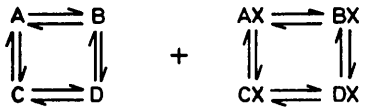

SCHEME 2

This considerably reduced the computational problem. Before computing the E–Me band shapes, the static parameters, namely chemical shifts, ^3J(Pt–H) values, invertomer populations, and spin–spin relaxation times T_2^*, were measured as accurately as possible in a wide temperature range where the inversion process was slow. With the exception of certain chemical shifts, no strong temperature dependencies of these parameters were found (Table 2).

Experimental and simulated spectra of the S–Me region of [PtIMe$_3${MeS(CH$_2$)$_2$SMe}] are shown in Figure 2, where excellent agreement between both sets of line shapes will be noted showing that the assumption of single-site inversion of S atoms is very probably justified. However, to test whether synchronous double-site inversion could be clearly distinguished from the single-site process, attempts

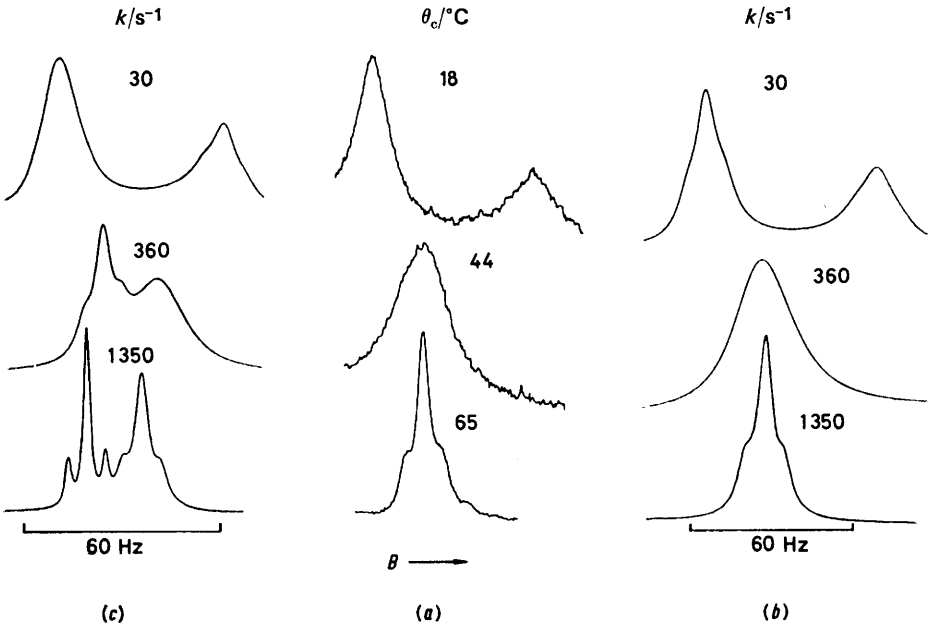

FIGURE 4 Intermediate-temperature spectra of the SMe region of [PtIMe$_3${MeS(CH$_2$)$_2$SMe}] showing how the experimental band shapes (*a*) can be explained in terms of a single site (*b*) rather than a synchronous double site (*c*) inversion mechanism

were made to simulate certain of the experimental spectra according to Scheme 3 which allows only interconversion of the two DL isomers and of the two *meso* isomers. Typical results of these fittings are depicted in Figure 4. It will be seen that at higher temperatures where the inversion is quite rapid the fittings are very poor since the double inversion process leads to *two* averaged chemical shifts and not one averaged shift as is observed. It can therefore be concluded that synchronous double inversion is *not* the dominant process, and the spectral changes can be fully accounted for on the basis of inversion at individual E atoms.

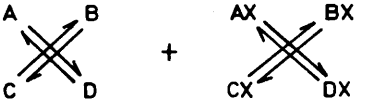

SCHEME 3

In the six-membered ring complexes [PtXMe$_3${MeS-(CH$_2$)$_3$SMe}] only one of the *meso* isomers was detected. This was presumably a result of either very low abundance of the other isomer or of fortuitous chemical-shift overlap

with the DL signals. The former explanation seems the more reasonable. The spectral changes observed for the six-membered ring complexes were very analogous to the corresponding five-membered ring complexes suggesting that the same rate process was being monitored. However, in the six-membered ring complexes both the possibilities of chair-to-chair ring reversal and pyramidal site inversion of E atoms have to be considered. The ring reversal process is likely to be a relatively low-energy process and evidence for it was sought by cooling the complexes as low as the solvent and spectrometer allowed, *ca.* −80 °C. However, no further changes in the spectra were observed implying *either* that the ring reversal process was always fast on the n.m.r. time scale of observation *or* that the ring appeared conformationally rigid from the n.m.r. viewpoint as a result of only one of the two possible conformers I and II being thermodynamically favoured. Conformer I would seem to be more favoured from the point of view of interactions of the platinum methyls with the chelate ring. Such a structure would be compatible with our non-detection of one of the *meso* isomers (presumably *meso*-2 with both methyls *trans* to X) since this isomer would involve considerable E–Me · · · E–Me and E–Me · · · Pt–Me interactions. It is pertinent to note here that *X*-ray structural analyses of $[W(CO)_4\{Bu^tS(CH_2)_nSBu^t\}]$ (n = 2 or 3) [21] show that the S · · · S non-bonded distance is 4.0 pm shorter in the six- compared to the five-membered ring

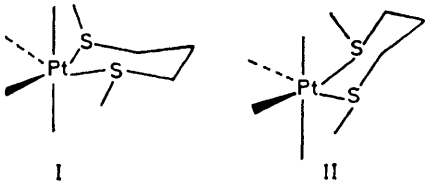

I II

complex. Thus, steric crowding appears to be a likely explanation of the non-detection of the *meso*-2 isomer. The observation of this isomer in the corresponding selenium complexes is in part attributable to the larger Pt–E bond distance which will reduce the E–Me · · · Pt–Me interactions. It should be noted that the population of the *meso*-1 isomer in the series $[PtXMe_3\{MeS(CH_2)_3SMe\}]$ varies with X in a reverse manner to the five-membered ring complexes. In this case the increasing size of the halogen appears to slightly favour *meso*-1 at the expense of the DL isomers. This different dependence may be related to the fact that these complexes do not possess pseudo-planar rings like the five-membered rings. The authors therefore conclude that the energy barrier due to six-membered ring reversal probably comes within the measurable n.m.r. range and would be detected if the conformer populations p_I and p_{II} were similar, but a very low-energy barrier cannot be ruled out on the basis of the experiments to date.

Typical experimental spectra of $[PtClMe_3\{MeS(CH_2)_3SMe\}]$ are shown in Figure 5. The computer-simulated spectra were based on the spin systems shown below where X denotes ^{195}Pt. The labels A, B, and C refer respectively to the methyls of the *meso*-1, DL-1, and DL-2 isomers of conformer I (or a time average of conformers I and II, *see* above). The numbering of the isomers is analogous to that of the five-membered ring complexes (Figure 1). Good agreement was achieved between observed and simulated spectra. The above spin system consisting of only three chemical configurations does not allow for the possibility of any synchronous double inversion. To test for this, it is necessary to compute the line shapes on the basis of *four* chemical configurations with the configuration due to the *meso*-2 isomer being given approximately zero abundance. This, however, was not carried out, it being considered highly unlikely that the inversion mechanism would differ significantly from the uncorrelated single-site process found for the five-membered ring complexes.

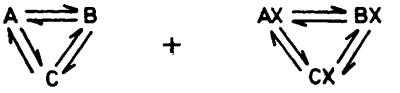

The results of the line-shape fittings for all the complexes are collected in Table 3. The values were calculated from the usual plots of ln k against T^{-1} and ln(k/T) against T^{-1} and are based on at least five, but more usually eight, fittings made over as wide a temperature range as possible, ($\Delta T \approx 60$ K). The errors are based on regression analyses of equally weighted graphical points. The inversion energies discussed below are based on rate constants, k, for the inversion process occurring in both directions. It would be physically more meaningful to calculate separate

TABLE 2

Static parameters of the complexes used in the DNMR band-shape program

	Meso-1 isomer				DL-isomers							*Meso*-2 isomer				
	ν_{AA} [a]/Hz				ν_B/Hz			ν_C/Hz				ν_{DD}/Hz				
Complex	a	b	^3J/Hz	p_{AA} [b]	a	b	^3J/Hz	a	b	^3J/Hz	p_{BC}	a	b	^3J/Hz	p_{DD}	T_2*/s
(1)	259.1	0.000	12.7	0.595	252.2	0.000	12.5	209.9	0.120	15.3	0.380	214.0	0.120	15.3	0.025	0.265
(2)	267.0	0.000	13.2	0.358	261.0	0.000	13.2	208.7	0.110	15.5	0.590	215.3	0.190	15.5	0.054	0.106
(3)	277.7	−0.024	13.9	0.295	272.9	−0.034	14.1	210.4	0.000	15.6	0.605	220.1	0.024	15.3	0.100	0.245
(4)	247.2	0.000	9.9	0.388	240.2	0.000	9.9	192.3	0.016	11.9	0.548	203.3	0.041	11.9	0.065	0.398
(5)	254.5	0.000	10.4	0.257	247.6	0.000	10.4	192.8	0.029	11.8	0.630	203.4	0.043	11.8	0.117	0.367
(6)	267.7	*c*	12.0	*c*	260.7	*c*	11.3	193.6	*c*	12.2	*c*	204.9	*c*	12.1	*c*	*c*
(7)	230.9	0.000	14.3	0.480	229.2	0.000	14.3	221.0	0.000	14.6	0.520					0.250
(8)	234.8	0.000	15.0	0.500	233.0	0.000	15.0	220.0	0.000	14.8	0.500					0.318
(9)	240.5	0.000	15.7	0.515	239.0	0.000	15.9	224.6	0.065	15.0	0.480					0.245
(10)	227.4	0.000	11.0	0.390	228.4	0.029	11.0	205.7	0.063	11.6	0.570	205.2	0.063	11.6	0.040	0.637
(11)	230.6	0.007	11.5	0.350	231.6	0.031	11.5	205.3	0.067	11.6	0.580	204.2	0.067	11.6	0.070	0.637
(12)	236.2	*c*	11.8	*c*	238.0	*c*	12.2	206.6	*c*	11.6	*c*	204.9	*c*	11.6	*c*	*c*

[a] Chemical shifts (ν_i) relative to $SiMe_4$ are given by ν_i/Hz = a − b(θ_c/°C). [b] Isomer populations (±0.005). [c] Not calculated.

energies for the *meso*→DL and the DL→*meso* processes. However, we have shown that the energies for these two

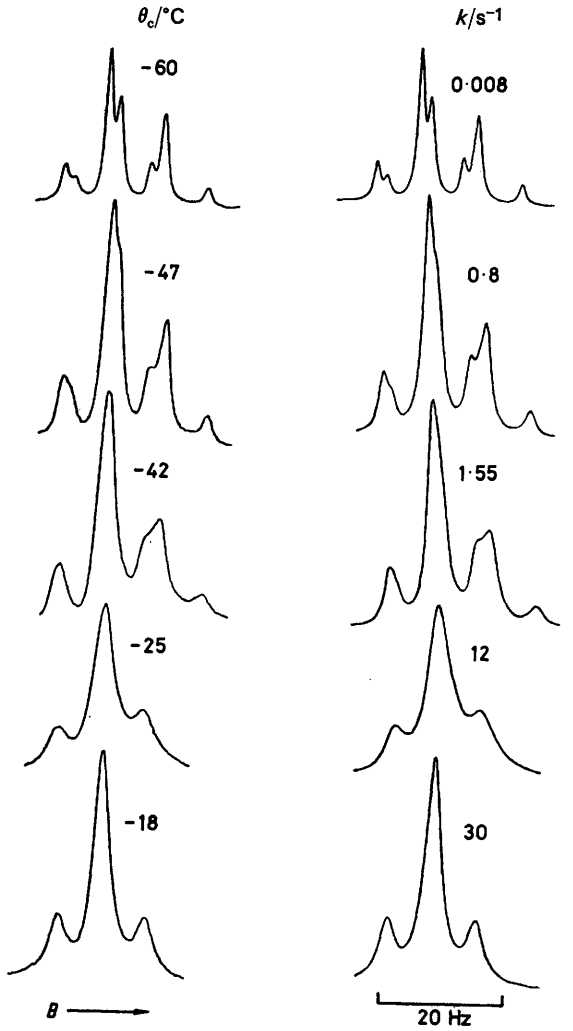

FIGURE 5 Variable-temperature ^1H n.m.r. spectra of the SMe region of $[PtClMe_3\{MeS(CH_2)_3SMe\}]$ and the computer-simulated spectra

different directions are very similar and, in general, differ by an amount comparable to (or less than) the calculated error of either value. It was therefore considered that no further insight into the nature of the inversion process would be gained by quoting separate energies for the two directions of each inversion process.

DISCUSSION

The Arrhenius and thermodynamic activation parameters (Table 3) clearly indicate that the inversion rates in these platinum(IV) complexes are extremely fast compared to those found in sulphoxides,[22] selenoxides,[23] thiosulphinates,[24] and sulphonium ions.[25] This is most probably due to back donation of platinum *d*-orbital electrons to sulphur or selenium *d*-orbitals in the transition state. It will be seen that the activation energy and the free energy of activation for inversion at Se atoms are 9—12 kJ mol^{-1} higher than for the corresponding sulphur complexes. A similar dependence on the nature of the chalcogen atoms has been noted previously in palladium and platinum chelate complexes [11,17] and in complexes with unidentate S and Se ligands.[6,26] The increase in activation energy is thought to relate primarily to the increase in *s* character of the lone pair on the chalcogen atom in the series S→Se→Te.

Table 3 clearly indicates a decrease in barrier height as the heterocyclic ring size increases from five to six. For example, $\Delta G^{\ddagger}$ is 5—6 kJ mol^{-1} lower for six-membered than for the analogous five-membered ring complexes. The trend mirrors that found for inverting nitrogen atoms when incorporated in various sized rings [4] and is almost certainly attributable to a stabilisation of the transition state compared to the ground state by an amount related to the angle constraint. The increase in barrier energy on going from S to Se in the six-membered ring complexes is particularly noteworthy since it rules out the possibility that the rate process being detected here is ring reversal. The barrier energy of the latter process is expected to *decrease* from S to Se as exemplified by 1,3-dithiane [27] ($\Delta G^{\ddagger} = 43.1$ kJ mol^{-1}) and 1,3-diselenane [28] ($\Delta G^{\ddagger} = 34.2$ kJ mol^{-1}). Such a trend is opposite to that observed here.

No obvious dependence of barrier energies on the nature of the halogen was found, suggesting that any *cis* influence of halogen is not pronounced. Similarly equivocal results for halogen dependence have been reported previously.[6]

For purely intramolecular rate processes, such as the thermal inversion process where no dissociation occurs in the transition state, $\log_{10}A$ should be *ca.* 13 and $\Delta S^{\ddagger}$ *ca.* 0 J K^{-1} mol^{-1}. Our results are in general agreement with this. Further evidence supporting a purely intramolecular process comes from the observation of

TABLE 3

Arrhenius and activation parameters for sulphur and selenium inversion in complexes of trimethylplatinum(IV) halides

Complex	E_a/kJ mol^{-1}	$\log_{10}A$	$\Delta G^{\ddagger}$/kJ mol^{-1}	$\Delta H^{\ddagger}$/kJ mol^{-1}	$\Delta S^{\ddagger}$/J K^{-1} mol^{-1}
(1)	63.4 ± 0.7	12.8 ± 0.1	63.3 ± 1.4	61.0 ± 0.7	−7.7 ± 2.4
(2)	69.8 ± 2.2	14.0 ± 0.4	62.8 ± 4.4	67.4 ± 2.2	15.5 ± 7.5
(3)	66.9 ± 2.0	13.5 ± 0.3	62.6 ± 3.9	64.4 ± 2.0	5.9 ± 6.5
(4)	74.4 ± 3.4	13.2 ± 0.6	72.2 ± 6.6	71.7 ± 3.4	−1.4 ± 10.8
(5)	77.3 ± 4.2	13.6 ± 0.7	72.4 ± 8.0	74.6 ± 4.2	7.3 ± 13.0
(7)	59.0 ± 2.0	13.5 ± 2.0	55.0 ± 5.0	57.0 ± 2.0	7.0 ± 9.0
(8)	56.0 ± 1.0	12.7 ± 0.2	56.6 ± 2.3	54.0 ± 1.0	−8.9 ± 4.1
(9)	64.4 ± 1.1	14.3 ± 4.3	55.8 ± 2.3	62.4 ± 1.1	22.1 ± 4.3
(10)	68.8 ± 4.0	13.3 ± 0.7	66.0 ± 8.0	66.3 ± 4.0	1.0 ± 13.6
(11)	66.2 ± 4.6	12.8 ± 0.8	66.2 ± 9.4	64.0 ± 4.7	−8.2 ± 16.0

averaged ^3J(Pt–H) couplings above the coalescence temperatures of all the complexes studied. Any appreciable dissociation–recombination process would remove such couplings.

We acknowledge the technical assistance of Mr. E. Underwood in obtaining many of the spectra.

[9/1558 *Received*, 1*st October*, 1979]

REFERENCES

[1] A. T. Bottini and J. D. Roberts, *J. Amer. Chem. Soc.*, 1956, **78**, 5126.
[2] H. Kessler, *Angew. Chem.*, 1970, **9**, 219.
[3] A. Rauk, L. C. Allen, and K. Mislow, *Angew. Chem.*, 1970, **9**, 400.
[4] J. B. Lambert, *Topics Stereochem.*, 1971, **6**, 19.
[5] E. W. Abel, R. P. Bush, F. J. Hopton, and C. R. Jenkins, *Chem. Comm.*, 1966, 58.
[6] E. W. Abel, G. W. Farrow, K. G. Orrell, and V. Šik, *J.C.S. Dalton*, 1977, 42; E. W. Abel, A. K. Ahmed, G. W. Farrow, K. G. Orrell, and V. Šik, *ibid.*, p. 47.
[7] E. W. Abel, G. W. Farrow, and K. G. Orrell, *J.C.S. Dalton*, 1976, 1160.
[8] P. Haake and P. C. Turley, *J. Amer. Chem. Soc.*, 1967, **89**, 4611.
[9] P. C. Turley and P. Haake, *J. Amer. Chem. Soc.*, 1967, **89**, 4617.
[10] G. Hunter and R. C. Massey, *J.C.S. Dalton*, 1976, 2007 and refs. therein.
[11] R. J. Cross, T. H. Green, and R. Keat, *J.C.S. Dalton*, 1976, 1150 and refs. therein.
[12] E. W. Abel, A. R. Khan, K. Kite, K. G. Orrell, and V. Šik, *J. Organometallic Chem.*, 1978, **145**, C18.
[13] E. W. Abel, A. R. Khan, K. Kite, K. G. Orrell, and V. Šik, preceding paper.
[14] J. Laane, in ' Vibrational Spectra and Structure,' ed. J. R. Durig, Marcel Dekker, New York, 1972, vol. 1, p. 25.
[15] D. A. Kleier and G. Binsch, *J. Magn. Reson.*, 1970, **3**, 146; D. A. Kleier and G. Binsch, DNMR3, Program 165, Quantum Chemistry Program Exchange, Indiana University, 1970.
[16] D. Höfner, S. A. Lesko, and G. Binsch, *Org. Magn. Reson.*, 1978, **11**, 179.
[17] R. J. Cross, I. G. Dalgleish, G. J. Smith, and R. Wardle, *J.C.S. Dalton*, 1972, 992.
[18] W. Kitching, C. J. Moore, and D. Doddrell, *Inorg. Chem.*, 1970, **9**, 541.
[19] A. D. Buckingham and P. J. Stevens, *J. Chem. Soc.*, 1964, 4583.
[20] A. J. Cheney and B. L. Shaw, *J. Chem. Soc.* (*A*), 1971, 3545.
[21] G. M. Reisner, I. Bernal, and G. R. Dobson, *J. Organometallic Chem.*, 1978, **157**, 23.
[22] D. R. Rayner, A. J. Gordon, and K. Mislow, *J. Amer. Chem. Soc.*, 1968, **90**, 4854.
[23] M. Oki and H. Iwamura, *Tetrahedron*, 1966, 217.
[24] P. Koch and A. Favor, *J. Amer. Chem. Soc.*, 1968, **90**, 3867.
[25] D. Darwish and R. L. Tomilson, *J. Amer. Chem. Soc.*, 1968, **90**, 5938.
[26] J. C. Barnes, G. Hunter, and M. W. Lown, *J.C.S. Dalton*, 1976, 1227.
[27] H. Friebolin, H. G. Schmid, S. Kabuss, and W. Faisst, *Org. Magn. Reson.*, 1969, **1**, 67.
[28] A. Geens, G. Swaelens, and M. Anteunis, *Chem. Comm.*, 1969, 439.